

Magnetic and magnetoimpedance studies on controlled Joule annealed amorphous Co₇₃Fe_{4.5}Ni_{0.5}Mn_{0.5}Nb_{0.5}Si_{4.2}B_{16.8} alloy

Subhendu Kumar Manna and V. Srinivas

Citation: *Journal of Applied Physics* **115**, 17A324 (2014); doi: 10.1063/1.4865767

View online: <http://dx.doi.org/10.1063/1.4865767>

View Table of Contents: <http://scitation.aip.org/content/aip/journal/jap/115/17?ver=pdfcov>

Published by the *AIP Publishing*

Articles you may be interested in

Cryogenic Joule annealing induced large magnetic field response of Co-based microwires for giant magnetoimpedance sensor applications

J. Appl. Phys. **116**, 053907 (2014); 10.1063/1.4892042

The effect of field-quenching fabrication on the magnetoimpedance response in Co₆₆Fe₄Ni₁Si₁₅B₁₄ amorphous ribbons

J. Appl. Phys. **111**, 053913 (2012); 10.1063/1.3687417

Improvement of soft magnetic properties of [(Fe 0.5 Co 0.5) 0.75 B 0.20 Si 0.05] 96 Nb 4 bulk metallic glass by B₂O₃ flux melting

J. Appl. Phys. **103**, 07E702 (2008); 10.1063/1.2829012

Structural, magnetic, and magnetostriction behaviors during the nanocrystallization of the amorphous Ni 5 Fe 68.5 Si 13.5 B 9 Nb 3 Cu 1 alloy

J. Appl. Phys. **99**, 08F104 (2006); 10.1063/1.2162810

Permeability and giant magnetoimpedance in Co 69 Fe 4.5 X 1.5 Si 10 B 15 (X=Cr , Mn, Ni) amorphous ribbons

J. Appl. Phys. **89**, 7218 (2001); 10.1063/1.1359226



Not all AFMs are created equal
Asylum Research Cypher™ AFMs
There's no other AFM like Cypher

www.AsylumResearch.com/NoOtherAFMLikeIt

OXFORD
INSTRUMENTS
The Business of Science®

Magnetic and magnetoimpedance studies on controlled Joule annealed amorphous $\text{Co}_{73}\text{Fe}_{4.5}\text{Ni}_{0.5}\text{Mn}_{0.5}\text{Nb}_{0.5}\text{Si}_{4.2}\text{B}_{16.8}$ alloy

Subhendu Kumar Manna and V. Srinivas^{a)}

Department of Physics, Indian Institute of Technology Madras, Chennai 600036, India

(Presented 8 November 2013; received 23 September 2013; accepted 8 November 2013; published online 13 February 2014)

We report magnetic and magnetoimpedance (MI) properties of as-quenched and Joule annealed (with and without external magnetic field) amorphous $\text{Co}_{73}\text{Fe}_{4.5}\text{Ni}_{0.5}\text{Mn}_{0.5}\text{Nb}_{0.5}\text{Si}_{4.2}\text{B}_{16.8}$ alloy composition. The Joule annealing in the presence of magnetic field induces not only surface microstructural changes but also favourable anisotropy. Dc magnetic measurements show controlled annealing enhances soft magnetic nature of the sample. Virgin ribbons show $M_S \sim 125$ emu/g with $\mu_r \sim 10^4$ and exhibit large MI ratio of $\sim 100\%$ at 3 MHz frequency. This MI ratio was further enhanced to 152% on Joule annealing (current density 0.85×10^7 A/m²) in the presence of applied magnetic field of 500 Oe. The field dependence MI shows a double-peak feature in as-spun ribbons, which is significantly enhanced for field annealed (FA) samples. The enhancement in MI and magnetic field sensitivity (η) in FA amorphous ribbons is attributed to the development of nanograins on the surface layer that strengthens the transverse magnetic structure.

© 2014 AIP Publishing LLC. [<http://dx.doi.org/10.1063/1.4865767>]

I. INTRODUCTION

Rapidly solidified Co-based alloys that possess nearly zero magnetostriction (λ) are expected to exhibit soft magnetic properties. These properties are further enhanced by tuning the microstructure through controlled annealing in the presence of magnetic field.^{1–3} In particular, for smaller magnetostriction alloys the easier magnetic anisotropy is expected during magnetic field annealing (FA). Marín *et al.*, showed that the nucleated nanograins can be aligned in the magnetic field direction during their initial stages of growth from the amorphous matrix under FA.⁴ Since Joule annealing (JA) requires shorter annealing time to achieve finer control of microstructure compared to the conventional furnace annealing, this method is suitable for amorphous ribbons to study the evolution of microstructure and related properties. Further from the view point of improving controllability of the permeability, JA in the presence of magnetic field is well known method that can generate magnetic anisotropy suitable for magnetic sensor applications. Such materials exhibit large variations in skin depth [$\delta = (2/\sigma\mu f)^{1/2}$ where σ , μ , and f are electrical conductivity, permeability, and frequency respectively]⁵ at higher frequencies which in turn produces large variation in their impedance value on application of small magnetic fields. In fact, higher sensitivity and giant magnetoimpedance (GMI) was reported in Co-rich amorphous alloys.^{6–9} The FA of amorphous ribbon can either enhance or destroy GMI property depending on the direction of field applied during annealing.^{3,10} Tang *et al.*, suggested that FA can generate graded microstructure along the cross section of the ribbon, featuring amorphous-phased skin-layers and/or nanocrystalline amorphous composite layer.¹¹ They further suggest that developed microstructure is sensitive to the direction of applied magnetic field during FA.

Such microstructures can induce unique electrical magnetic properties that are different from traditional amorphous species. Although amorphous ribbons with composition close to $\text{Co}_{70}\text{Fe}_5\text{Si}_{15}\text{Nb}_{2.2}\text{Cu}_{0.8}\text{B}_7$ show large MI values, the role of anisotropy/microstructure in relation to the GMI values are yet to be investigated.⁷ In this work, amorphous $\text{Co}_{73}\text{Fe}_{4.5}\text{Ni}_{0.5}\text{Mn}_{0.5}\text{Nb}_{0.5}\text{Si}_{4.2}\text{B}_{16.8}$ ribbons have been systematically Joule annealed under different annealing conditions to investigate the role of surface microstructure variations on magnetic and MI behaviour. We show that controlled FA can generate graded amorphous/nanocrystalline microstructure which enhances the MI and field sensitivity (η) of the sample.

II. EXPERIMENTAL DETAILS

Amorphous ribbons (2 mm wide, 44 ± 2 μm thick, and few meters long) were prepared by conventional arc melting and subsequent melt spinning techniques with a wheel speed of 37 m/s under argon atmosphere. As-quenched (AQ) ribbons were JA with a moderate current density 0.85×10^7 A/m² for 2–10 min under vacuum (10^{-3} millibar) to avoid possible surface oxidation of the samples. Further, the ribbons were subjected to similar heat treatment under the varying dc magnetic fields (applied perpendicular to length of the ribbon) of 50–5000 Oe for an optimum time period (6 min). The X-ray powder diffraction (XRD) confirms the amorphous nature of as-quenched ribbon. Magnetic parameters were evaluated using vibrating sample magnetometer (VSM) (Micro Sence EZ-9), Coercimeter (Model: CR/02), and a commercial B-H loop Tracer (Model: AMH-20K-S). Impedance measurements on 5 cm long ribbons were performed with HP 4192A impedance analyzer in the frequency range of 500 kHz–13 MHz by passing 10 mA alternating current. A magnetic field up to 100 Oe was applied along the length of the ribbons, using a Helmholtz coil. MI ratio and magnetic

^{a)}Electronic mail: veeturi@physics.iitm.ac.in.

field sensitivity(η) are defined as $MI\% = [(Z(H) - Z(H_{\max})) / Z(H_{\max})]\%$ and $\eta = (d/dH)(\Delta Z/Z)$, where $Z(H)$ and $Z(H_{\max})$ stand for the impedance in field H and in the maximum field $H_{\max} = 100$ Oe, respectively.

III. RESULTS AND DISCUSSION

The XRD patterns of AQ, JA, and FA ribbons show essentially an amorphous phase. The Differential Scanning Calorimetry (DSC) profile shows two widely separated exothermic peaks at 450°C (T_{x1}) and 572°C (T_{x2}), respectively, which suggests that there is two phase crystallization. The scanning electron microscope (SEM) micrographs of as-quenched and heat-treated ribbons are shown in Fig. 1, for (a) AQ, (b) 6 min JA, (c) 10 min JA, and (d) 500 Oe FA. The AQ ribbon exhibits almost featureless background, while development of nano size crystal with amorphous background could be seen in 6 min. JA sample and they further grow into bigger grains in the case of 10 min JA sample. Interestingly, 500 Oe FA sample shows the development of nanostructured well separated particles on the amorphous background, which is in agreement with the earlier reports.¹¹ Although SEM images show a clear evidence of surface crystallization, XRD patterns show amorphous nature which suggests that the Joule annealing modifies surface microstructure. These observations further suggest the existence of graded microstructure, i.e., surface nanocrystalline layer but the inner layers still remain in the amorphous state. Isothermal magnetization (M) curves as a function of field (H) at 300 K for AQ and annealed samples are shown in Fig. 2, which suggest the magnetization saturates ($M_s \sim 110$ – 130 emu/g) below 100 Oe for all the samples investigated. Coercivity (H_c) values are evaluated to be 0.061, 0.125, and 0.046 (± 0.01) Oe for AQ, 6 min JA, and 500 Oe FA samples, respectively. The frequency dependence of magnetic character of AQ ribbon was further investigated in the frequency range 50 Hz–20 kHz. It is observed that the initial permeability value reduced from 10^4 to 10^3 , while H_c and hysteresis loss increase with frequency (inset of Fig. 2). Figure 3 shows the variation of MI as a function of applied field (H) at four

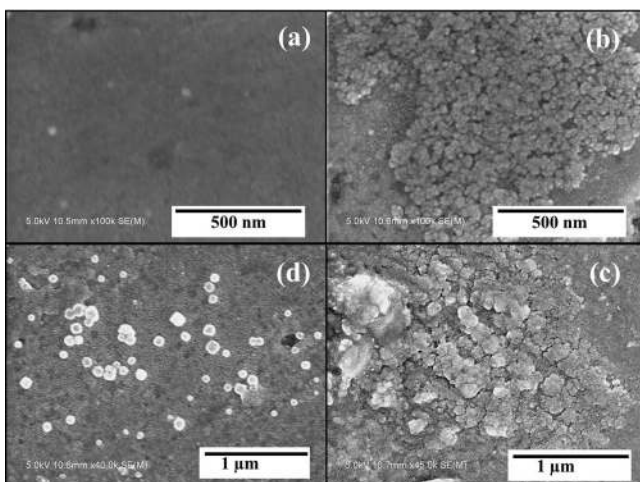


FIG. 1. SEM micrograph of (a) AQ, (b) 6 min JA, (c) 10 min JA, and (d) 500 Oe FA ribbons.

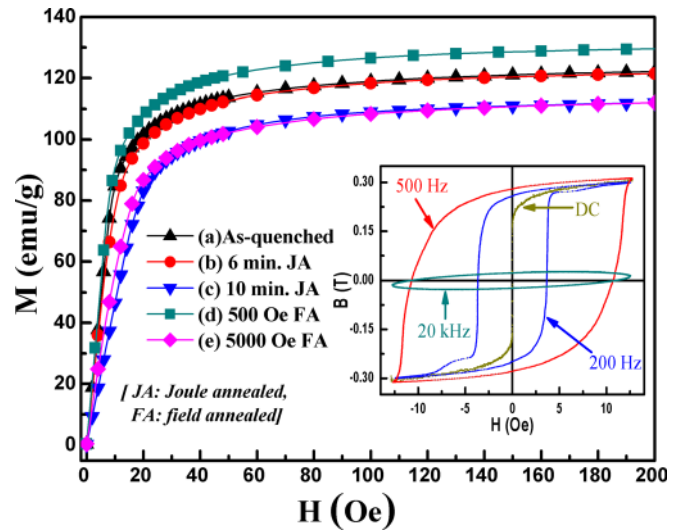


FIG. 2. M-H curves at 300 K for (a) AQ, (b) 6 min JA, (c) 10 min JA, (d) 500 Oe FA, and (e) 5000 Oe FA ribbons. Inset: B-H loop of as-quenched ribbon at different frequencies.

different frequencies for (a) AQ, (b) 6 min JA, (c) 10 min JA, (d) 500 Oe FA, and (e) 5000 Oe FA ribbons. The following features can be noticed from the figure: (i) As JA time is increased the maximum MI has been observed in 6 min samples suggesting it to be an optimum time at this current density. (ii) Similarly, 500 Oe FA exhibits maximum MI of $\sim 152\%$. (iii) MI initially increases with H and goes through

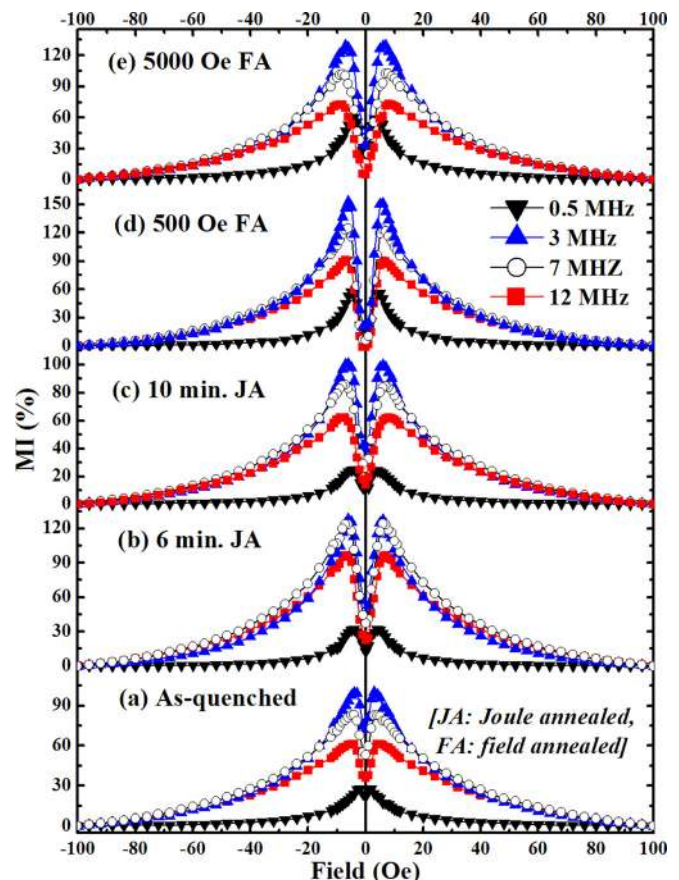


FIG. 3. Variation of MI with magnetic field for (a) as-quenched, (b) 6 min JA, (c) 10 min JA, (d) 500 Oe FA, and (e) 5000 Oe FA ribbons.

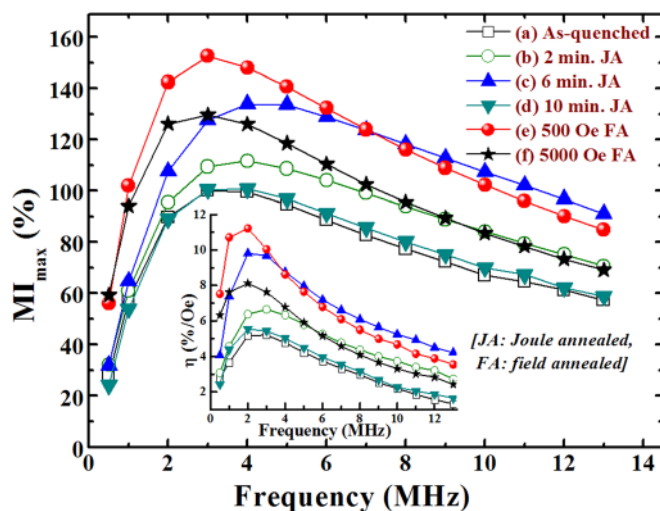


FIG. 4. MI_{\max} and magnetic field sensitivity (η) (Inset) variations with frequency for (a) AQ, (b) 2 min JA, (c) 6 min JA, (d) 10 min JA, (e) 500 Oe FA, and 5000 Oe FA ribbons.

a maximum (MI_{\max}) at certain applied field (H_k). The double peak behaviour of MI with field for all samples suggests the presence of transverse magnetic domains.⁵ Further, the H_k varies with annealing condition at particular frequency and follows H_c . These observations confirm that the transverse anisotropy can be tuned through JA and FA for Co-based amorphous ribbons, which is in agreement with earlier work.^{1,7,8} Similar behaviour was also reported in Co coated CoFeZrB amorphous ribbons and attributed to reduction in stray fields due to surface irregularities and the enhanced magnetic flux paths closure.¹² Fig. 4 shows the frequency dependence of MI_{\max} %, which increases with frequency up to ~ 3 MHz and then decreases for all samples which could be due to dominant domain wall pinning at higher frequency.⁵ Inset of Fig. 4 represents the variation of field sensitivity (η) with frequency for all samples. A maximum η % of 11.2% at 2 MHz has been obtained for 500 Oe FA ribbon, which is large compared to a AQ ribbon.

From above observations and earlier reports, we believe the large MI% in virgin sample is due to the fine tuning of composition which results in higher permeability. However, controlled JA or FA improved the μ (or susceptibility in Fig. 2) and σ due to stress relaxation/surface nanocrystallization.¹¹ Thus, developing a large variation in skin depth and hence in MI. These changes in magnetic and electrical properties can be attributed to possible gradient structure from surface to interior of the ribbon as shown in the micrographs. A significant variation in microstructure in JA and FA also suggests that in the 500 Oe FA sample an optimum sized nanocrystals (ncs) develop to minimize the anisotropy (due

to random anisotropy) and enhance the μ (reduce H_c). However, prolonged JA or FA either creates agglomerates of ncs (compared to magnetic exchange length) or larger crystals where crystalline anisotropy dominates, which in turn results in deterioration of MI%. It is important to point out here that Phan *et al.*, observed single peak behaviour in MI vs H curves in Co-rich alloys as opposed to present and earlier investigations.¹² These observations suggest presently studied samples have transverse magnetic structure of AQ state. Further, the transverse magnetic structure builds up under FA compared to as quenched state of the ribbon. From the perspective of sensor applications, present studies demonstrate a way to systematically tailor the magnetic properties to obtain superior GMI with better field sensitivity.

IV. SUMMARY AND CONCLUSIONS

We have systematically investigated the effects of Joule and field annealing on magnetic and magnetoimpedance properties of amorphous $Co_{73}Fe_{4.5}Ni_{0.5}Mn_{0.5}Nb_{0.5}Si_{4.2}B_{16.8}$ ribbons. A soft magnetic character and large MI ratio of AQ ribbons suggests that both composition as well as quality of surface skin layer play significant role. It is also demonstrated magnetic field annealing for an optimum time assists in enhancing not only MI ratio but also field sensitivity. From the application point of view FA samples exhibit better MI and field sensitivity in the frequency range 0.5–10 MHz.

ACKNOWLEDGMENTS

The authors acknowledge Professor K. Balasubramanian, Department of Mechanical Engineering, Indian Institute of Technology Madras, Chennai for allowing use of impedance analyzer.

- ¹A. Chaturvedi, N. Laurita, A. Leary, M.-H. Phan, M. E. McHenry, and H. Srikanth, *J. Appl. Phys.* **109**, 07B508 (2011).
- ²R. L. Sommer and C. L. Chien, *Appl. Phys. Lett.* **67**, 857 (1995).
- ³P. R. Ohodnicki, D. E. Laughlin, M. E. McHenry, V. Keylin, and J. Huth, *J. Appl. Phys.* **105**, 07A322 (2009).
- ⁴P. Marín, M. López, A. Vlad, A. Hernando, M. L. Ruiz-González, and J. M. González-Calbet, *Appl. Phys. Lett.* **89**, 033508 (2006).
- ⁵M. H. Phan and H. X. Peng, *Prog. Mater. Sci.* **53**, 323 (2008).
- ⁶L. V. Panina and K. Mohri, *Appl. Phys. Lett.* **65**, 1189 (1994).
- ⁷M. H. Phan and H. X. Peng, *J. Appl. Phys.* **99**, 08C505 (2006).
- ⁸L. Gonzalez-Legarreta, V. M. Prida, B. Hernando, M. Ipatov, V. Zhukova, A. P. Zhukov, and J. Gonzalez, *J. Appl. Phys.* **113**, 053905 (2013).
- ⁹A. Ruiz, D. Mukherjee, J. Devkota, M. Hordagoda, S. Witanachchi, P. Mukherjee, H. Srikanth, and M. H. Phan, *J. Appl. Phys.* **113**, 17A323 (2013).
- ¹⁰S. Atalay, *Physica B* **368**, 273 (2005).
- ¹¹Z. Tang, Y. Song, Q. Sun, T. Zhang, and Y. Jiang, *Nanoscale* **4**, 386 (2012).
- ¹²N. Laurita, A. Chaturvedi, C. Bauer, P. Jayathilaka, A. Leary, C. Miller, M.-H. Phan, M. E. McHenry, and H. Srikanth, *J. Appl. Phys.* **109**, 07C706 (2011).